minerals

MDPI

Article

Geochemical Characterization and Process Response of Coal-Derived Post-Mining Waste to Dry Electrostatic and Magnetic Separation: Implications for REE Pre-Concentration Screening

Paweł Friebe [1,*], Rafał Baron [1], Daniel Kowol [1], Piotr Matusiak [1], Olga Ziółkowska [1], Agata Czardybon [2] and Karina Ignasiak [2]

[1] KOMAG Institute of Mining Technology, Pszczyńska 37, 44-101 Gliwice, Poland; rbaron@komag.eu (R.B.); dkowol@komag.eu (D.K.); pmatusiak@komag.eu (P.M.); oziolkowska@komag.eu (O.Z.)
[2] Institute of Energy and Fuel Processing Technology, Zamkowa 1, 41-803 Zabrze, Poland; aczardybon@itpe.pl (A.C.); kignasiak@itpe.pl (K.I.)
* Correspondence: pfriebe@komag.eu

Abstract

This study compares the response of five coal-derived post-mining waste streams from Poland and the Czech Republic to dry electrostatic and magnetic separation, with emphasis on rare earth element (REE) enrichment, product yield, and material variability. The materials included dump-derived wastes and process-derived streams from beneficiation operations. Electrostatic separation was performed on the <45 µm fraction, whereas magnetic separation was performed on the <3 mm fraction. Chemical composition was determined by ICP–MS, and process response was evaluated using enrichment factor (EF), product yield, and mass distribution. The ΣREE content of the feeds ranged from 109.33 to 250.54 ppm, while loss on ignition varied from 12.5% to 50.8%, confirming substantial heterogeneity. Electrostatic separation produced only moderate and material-specific enrichment, with EF ΣREE values generally close to unity and reaching a maximum of 1.26 for the Haldex K conductive product. Magnetic separation was less favourable, as most magnetic products showed ΣREE depletion or very low yields. Although the Haldex K paramagnetic product reached EF ΣREE = 1.30, its yield was only 0.2%. Overall, no tested configuration combined high REE enrichment with high product yield, indicating limited standalone beneficiation potential for the investigated materials. This study provides a comparative process-response assessment of low-grade, heterogeneous coal-derived post-mining waste streams and shows that dry electrostatic and magnetic separation can reveal material-dependent REE partitioning behaviour under laboratory conditions.

Keywords: coal mining waste; dry separation; electrostatic separation; magnetic separation; REE recovery; enrichment factor; beneficiation

Academic Editors: Ilhwan Park, Theerayut Phengsaart, Carlito Tabelin, Mayumi Ito and Weiran Zuo

Received: 28 April 2026
Revised: 31 May 2026
Accepted: 1 June 2026
Published: 4 June 2026

1. Introduction

The increasing demand for critical raw materials, including rare earth elements (REE), has intensified research into secondary and alternative sources of these elements. Mining and mineral-processing wastes are increasingly considered in this context, not only as environmental liabilities but also as potential anthropogenic resources within circular economy strategies. In this context, the evaluation of coal-derived post-mining waste requires not

only the determination of bulk REE concentrations, but also an assessment of whether REE-bearing components show preferential partitioning during physical separation. This study therefore combines ICP–MS-based chemical characterization with laboratory-scale dry electrostatic and magnetic separation tests to evaluate material-dependent process response.

1.1. Demand for Critical Raw Materials and Circular Economy Context

The development of clean energy technologies, electrified transport, permanent magnets, advanced electronics, and grid infrastructure has increased the strategic importance of REE and other critical raw materials (CRM). Recent analyses indicate sustained growth in demand for these elements, particularly in sectors linked to the energy transition and high-performance material supply chains [1–4].

From the European perspective, this demand is accompanied by a high dependence on geographically concentrated extraction and processing capacities. In response, the European Union has introduced policy and regulatory frameworks aimed at strengthening raw material security and increasing the role of secondary sources. Regulation (EU) 2024/1252 explicitly promotes the recovery and recycling of critical raw materials, including the development of secondary supply streams [5,6]. This is consistent with broader circular economy objectives and Sustainable Development Goal 12, which emphasize resource efficiency, waste reduction, and responsible production and consumption [7,8]. In this context, post-mining waste streams may contribute to both waste management and raw material security, provided that their composition and process response are sufficiently understood [5,9,10].

1.2. Mining Waste as a Potential Source of REE

Coal-derived post-mining waste represents an important category of secondary material in Central Europe because of the scale, spatial distribution, and long-term environmental relevance of historical and current coal-mining activities. In Poland and in the Czech part of the Upper Silesian Coal Basin, large volumes of processing waste have been deposited in dumps or managed in beneficiation facilities. These materials differ in origin, processing history, particle-size distribution, mineral composition, and organic matter content, which may strongly affect their behaviour during physical separation [11–14].

The present study was designed as a regional comparative case study focused on five coal-derived post-mining waste streams from Poland and the Czech Republic. The materials were selected intentionally rather than randomly. The selection criteria included the following: (i) location within the Upper Silesian Coal Basin or its industrial surroundings, (ii) different origins of the waste streams, including dump-derived materials and products or by-products of beneficiation operations, (iii) expected variability in particle-size distribution, mineral composition, organic matter content, and processing history, and (iv) availability of representative bulk samples suitable for laboratory-scale separation tests. The selected materials provide a controlled comparative set of waste streams with different origins, processing histories and material characteristics. This design enables assessment of how these differences affect REE distribution and the response to dry electrostatic and magnetic separation.

Coal-derived wastes are commonly dominated by aluminosilicate phases, accompanied by iron-bearing minerals, carbonaceous matter, carbonates, and accessory minerals. In the investigated materials, preliminary chemical characterization indicated that SiO_2 and Al_2O_3 are the dominant major oxides, with variable contributions of Fe_2O_3, CaO, MgO, alkali metal oxides, and loss on ignition [15,16]. Such variability is relevant because REE in coal and coal-related by-products usually occur at low concentrations and may be associated with several mineral hosts, including accessory phosphates, heavy minerals,

fine-grained aluminosilicates, or surface-bound phases [17,18]. Consequently, the beneficiation potential of these wastes cannot be assessed solely on the basis of bulk REE content. It is also necessary to determine whether REE-bearing components show preferential partitioning into products formed according to differences in electrical properties or magnetic susceptibility.

1.3. Separation Methods and Scope of the Study

Hydrometallurgical and bio-based extraction methods are being widely investigated for REE recovery from coal-derived wastes and fly ash, and they remain important routes for obtaining dissolved REE from low-grade secondary resources [17–19]. However, the direct application of dissolution-based methods to heterogeneous, low-grade post-mining wastes may involve high reagent consumption, partial dissolution of major matrix components, generation of liquid waste streams, and the need for multi-stage purification. For this reason, physical separation may be considered as a preliminary beneficiation or process-diagnostic stage rather than as a direct substitute for chemical leaching or bioleaching.

Dry electrostatic and magnetic separation were selected in this study because they respond to different material properties. Electrostatic separation exploits differences in conductivity, charge retention, and dielectric behaviour of particles, while magnetic separation is based on differences in magnetic susceptibility, particularly the response of iron-bearing and other magnetically susceptible phases [20–22]. These methods may therefore provide information on whether REE-bearing components are preferentially associated with electrically or magnetically distinguishable fractions. This is relevant for preliminary process-route design, especially when the objective is to reduce the mass of material directed to subsequent extraction stages or to identify whether further beneficiation is justified [16,17,20–22].

Recent studies on coal-derived materials and coal combustion by-products indicate that REE may occur in several associations, including aluminosilicate or glassy components, discrete phosphate or silicate minerals, Fe-bearing phases, and organic or carbon-rich matter [18,23,24]. Consequently, bulk REE concentration alone does not determine whether a material will respond favourably to physical separation. The response to electrostatic or magnetic separation depends on whether REE-bearing components are sufficiently liberated and whether they are associated with particles exhibiting distinct electrical or magnetic properties.

The feasibility of dry separation depends on local operating conditions, including electricity costs, water availability, product yield, separation selectivity and downstream processing requirements. Because no techno-economic or life-cycle assessment was performed, economic and environmental feasibility is outside the scope of this study.

The main contribution of this work is a comparative process-response assessment of five coal-derived post-mining waste streams from the Upper Silesian Coal Basin region and its industrial surroundings. This study combines ICP–MS-based REE determination with dry electrostatic and magnetic separation tests to evaluate the relationship between feed characteristics, product yield, enrichment factor and REE partitioning behaviour. This approach allows apparent concentration increases to be distinguished from process-relevant enrichment and identifies the limitations of dry physical separation as a preliminary screening step for low-grade, heterogeneous materials.

2. Materials and Methods

2.1. Materials and Sampling

Five coal-derived post-mining waste streams were selected for the study according to their origin, processing history, and expected material variability. Two materials were

collected from waste dumps located in the Czech Republic, i.e., Paskov and Karviná, while three materials were obtained from the Haldex facility in Poland: material from the Panewnicka dump ("Haldex S"), beneficiation waste ("Haldex O"), and beneficiation concentrate ("Haldex K"). This selection allowed the comparison of dump-derived materials with process-derived streams obtained during coal waste beneficiation. The general locations of the three dump-derived material sources are shown in Figures 1–3. For each material, one sampling point was selected within the corresponding material source area, and one bulk sample was collected for further preparation and laboratory testing.

Figure 1. General location of the Karviná post-mining waste material source area. The material was collected from one selected point within this location and used as a dump-derived coal-mining waste sample.

Figure 2. General location of the Panewnicka post-mining waste dump, corresponding to the Haldex S material. The material was collected from one selected point within this location and used as a dump-derived post-mining waste sample.

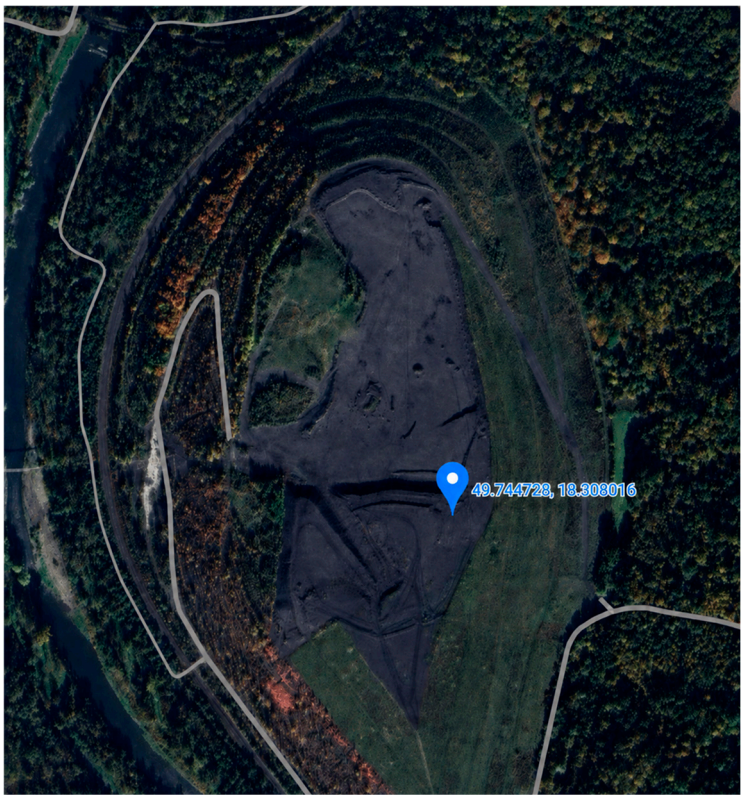

Figure 3. General location of the Paskov post-mining waste material source area. The material was collected from one selected point within this location and used as a dump-derived coal-mining waste sample.

Paskov and Karviná represent post-mining waste dumps in the Czech Republic, while Haldex S, Haldex O, and Haldex K represent material streams from the Haldex facility in Poland. For process-derived materials, the map indicates the facility location, whereas the material type is specified in the text.

The materials were selected to represent contrasting positions within the coal-waste management chain, including weathered dump-derived materials, secondary handled dump material, beneficiation waste and beneficiation concentrate. This selection enabled comparison of waste streams differing in origin, processing history, particle-size characteristics, mineral composition and organic matter content, all of which may influence REE distribution and separation behaviour.

Sampling was conducted during a single sampling campaign under stable meteorological conditions in order to minimize short-term variability related to moisture and surface conditions. For each material, one sampling point was selected within the corresponding material source area. The sampling procedure was generally consistent with the principles of ISO 18400-101:2017 for solid materials [25]. From the selected point, a bulk sample of approximately 100 kg was collected from the surface and shallow subsurface material.

The composite sampling strategy was adopted because post-mining waste materials are typically heterogeneous at both local and stockpile scales. The objective was to obtain representative bulk samples suitable for comparative chemical characterization and laboratory-scale separation tests. The collected samples were transported to the laboratory, dried, mechanically homogenized, and divided into representative laboratory test portions prior to particle-size preparation and separation.

After drying, each bulk sample was spread, mixed and repeatedly homogenized before subsampling. Representative portions for comminution and separation tests were obtained by successive sample splitting. The same preparation logic was applied to all

materials, including Haldex K. Therefore, the lower mass used for the Haldex K electrostatic separation tests should be interpreted as a representative laboratory test portion obtained from the homogenized bulk material, rather than as a separate grab sample. Nevertheless, because post-mining waste is inherently heterogeneous, the use of different feed masses is recognized as a methodological limitation when comparing absolute product masses between materials. All samples were processed as loose, granular coal-derived post-mining waste materials.

No chemical pre-treatment, pelletisation, slurry preparation, or flotation conditioning was applied before the separation tests. After drying and homogenization, the materials were mechanically prepared into two operational particle-size fractions: <3 mm for magnetic separation and <45 μm for electrostatic separation. The experimental system was therefore based on dry particulate feeds processed in laboratory-scale electrostatic and magnetic separators, with the operating parameters described in the following subsections.

2.2. Feed Preparation and Particle Size Classification

The experimental design was based on a comparative process-response evaluation of five post-mining waste streams subjected to two dry physical separation methods: electrostatic separation and magnetic separation. The main experimental factors were as follows:

(i) Material type;
(ii) Particle-size fraction;
(iii) Separation method;
(iv) Operating conditions of the separator;
(v) Product type obtained after separation.

For electrostatic separation, each material was tested under two operating conditions, referred to as Test I and Test II. The products were collected as conductive, semi-conductive, and non-conductive fractions. For magnetic separation, the materials were processed under different magnetic field intensity settings, and the products were collected as magnetically susceptible and non-magnetic fractions. In selected configurations, the magnetically susceptible product was further separated into strongly and weakly paramagnetic fractions.

The workflow of the experimental procedure was as follows:

- Collection of five bulk composite samples;
- Drying, homogenization, and representative subsampling;
- Preparation of the <3 mm fraction for magnetic separation;
- Additional grinding of representative portions to <45 μm for electrostatic separation;
- Dry electrostatic and magnetic separation tests;
- Weighing of separation products and calculation of mass yields and mass balance;
- Chemical analysis of feed and product samples;
- Calculation of ΣREE, ΣLREE, ΣHREE, enrichment factors, and repeatability indicators.

The overall experimental workflow and the distinction between controlled variables, intentionally varied variables and evaluation indicators are summarized in Scheme 1.

The experimental program was designed as a comparative process-response study rather than as a full factorial optimization of separator operating parameters. Therefore, the primary comparison was made between materials and product types under predefined laboratory conditions. Within each separation method, the key operational variables were controlled as far as possible, including drying procedure, homogenization, particle-size fraction, feed rate, separator settings within a given test configuration, laboratory temperature and humidity, separator cleaning, and replicate testing. The intentionally varied factors were the material type, the electrode voltage configuration used during electrostatic separation, and the magnetic field intensity configuration used during magnetic separation.

Because electrostatic and magnetic separation rely on different physical mechanisms and require different operational feed-size ranges, the results were interpreted separately for each method and compared using relative indicators, especially product yield, mass closure, enrichment factor, LOI and the EF–yield relationship.

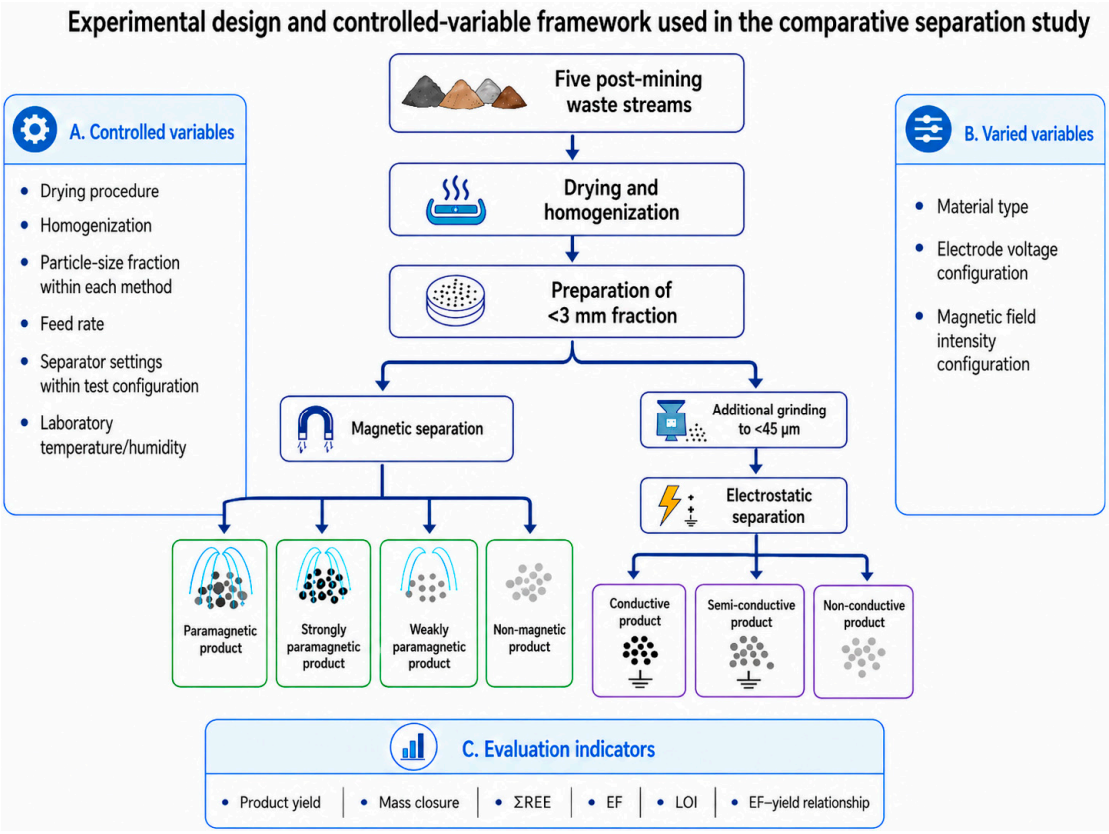

Scheme 1. Experimental design and controlled-variable framework used in the comparative separation study. The scheme shows the preparation of the five post-mining waste streams, the separation of the <3 mm fraction by magnetic separation, the additional grinding step to <45 µm before electrostatic separation, the resulting product groups, and the main controlled variables, varied variables and evaluation indicators used for process-response assessment.

The materials intended for dry separation tests were dried at 105 °C to constant mass, defined as a mass difference of less than 0.1% between two consecutive weighings, using a ZALMED SML48/250 laboratory dryer (Zalmed, Warsaw, Poland). After drying, the samples were cooled in a desiccator and homogenized before further preparation.

Two particle-size fractions were prepared because the two separation methods have different operating requirements and separation mechanisms. The material intended for magnetic separation was initially crushed using a Retsch BB100 jaw crusher (Retsch GmbH, Haan, Germany) with a 10 mm gap setting and subsequently ground using a Retsch DM200 disc mill (Retsch GmbH, Haan, Germany) to obtain the <3 mm fraction. Particle size was controlled using a Fritsch Pulverisette (FRITSCH GmbH, Idar-Oberstein, Germany) laboratory sieve shaker equipped with a 3 mm square mesh sieve, and the oversize fraction was returned to the mill.

A representative portion of the <3 mm material was then additionally ground for electrostatic separation using a Testchem LMW vibratory mill (Testchem Sp. z o.o., Zawiercie, Poland) to obtain the <45 µm fraction. Particle size after this stage was controlled using a Fritsch sieve shaker (Fritsch GmbH, Idar-Oberstein, Germany) equipped with a 45 µm square mesh sieve, and the oversize fraction was reprocessed.

The <45 μm particle-size fraction was selected for electrostatic separation as a fine and operationally stable feed suitable for the applied drum-type separator. Fine grinding was also intended to reduce the effect of coarse composite particles and improve the probability that differences in electrical behaviour between particle populations could be expressed during separation. This does not mean that electrostatic separation is limited to particles below 45 μm. Electrostatic separation may also be applied to coarser particles, depending on separator design, particle shape, surface properties, moisture content, and material composition.

In the present study, the <45 μm fraction was adopted as an operational feed size to ensure stable feeding, improve comparability between the investigated materials, and reduce the influence of coarse composite particles under laboratory-scale conditions. The cut-off was therefore selected for experimental and operational reasons, not because it had been confirmed as the liberation size of REE-bearing phases. The <45 μm fraction should not be interpreted as an experimentally confirmed liberation size of REE-bearing minerals. No microscopic liberation analysis, SEM-EDS, or XRD-based mineralogical quantification was performed in this study. Therefore, the actual liberation size of REE carriers was not determined.

The <3 mm fraction was selected for magnetic separation because it corresponded to the feed-size range suitable for the applied laboratory magnetic separator and allowed the response of the material to magnetic susceptibility differences to be assessed after moderate comminution. This size was not assumed to represent the liberation size of REE-bearing phases. Rather, it was used as an operational particle-size fraction enabling assessment of whether REE-bearing components are preferentially associated with magnetically susceptible particles in a relatively coarse feed.

Consequently, the <3 mm fraction was used as the feed for magnetic separation, whereas the <45 μm fraction was used as the feed for electrostatic separation. This distinction reflects the different technical requirements, feed-size suitability, and separation mechanisms of the two dry separation methods and should not be interpreted as evidence that REE liberation occurs at these particle sizes.

To minimize cross-contamination during crushing and grinding, a cleaning run was performed before the first sample and between subsequent samples. An inert material, pure quartz, was processed for 60 s, after which the equipment was cleaned using compressed air and isopropyl alcohol.

2.3. Electrostatic Separation

Electrostatic separation was carried out on the <45 μm fraction using a drum-type electrostatic separator (Boxmag Rapid Co. Ltd., Birmingham, UK) equipped with a high-voltage electrode and a three-compartment product collection system. The technical specifications of the separator are provided in Table S1. The general configuration of the electrostatic separator and the product collection system is shown in Scheme 2.

Two operating variants were applied for each material, as detailed in Table S2. These variants differed in drum rotational speed and electrode voltage, whereas the vibratory feeder setting and particle-size fraction were kept constant. The purpose of applying two operating configurations was to assess whether moderate changes in electrode voltage configuration and drum operation affected product distribution and REE enrichment.

The feed masses used for electrostatic separation are provided in Table S3. Different feed masses were used because the availability, handling behaviour and expected product distribution of the individual materials varied, and sufficient product mass was required for subsequent chemical analysis. In each case, the test portions were obtained from dried, homogenized and subsampled material. Particular attention was given to Haldex

K, for which lower feed masses were used. The 100 g Haldex K portions were obtained after drying, comminution, homogenization and successive subsampling of the prepared bulk material, rather than as separate grab samples. Therefore, the Haldex K test mass was considered representative for laboratory-scale process-response testing. However, the difference in feed mass between materials is acknowledged as a limitation for direct comparison of absolute product masses. For this reason, interpretation was based primarily on relative product yields, enrichment factors and repeatability indicators rather than on product mass alone.

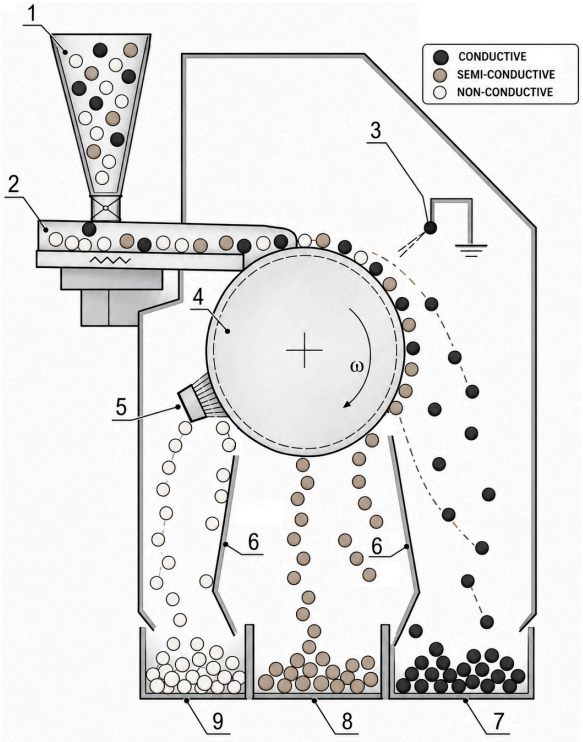

Scheme 2. Schematic representation of the drum-type electrostatic separator used in this study: 1—feed hopper; 2—vibratory feeder; 3—high-voltage electrode; 4—rotating drum; 5—brush; 6—separation partitions; 7—conductive product container; 8—semi-conductive product container; 9—non-conductive product container.

During electrostatic separation, the feed material was introduced from the hopper through the vibratory feeder onto the rotating drum as a thin layer at a constant feed rate of 10 g/min. The distance between the electrode and the drum surface was maintained at 0.03 m. In the electric field generated by the high-voltage electrode, particles followed different trajectories depending on their charging behaviour, discharge time and electrical properties. The products were collected as conductive, semi-conductive and non-conductive fractions in separate collection compartments, while the brush was used to remove particles remaining on the drum surface. Separation was conducted under controlled laboratory conditions, with temperature maintained at 22–24 °C and relative humidity at 45%–50%. Temperature and humidity were recorded at 10 min intervals. Between experimental series, the separator was cleaned using compressed air to minimize particle carry-over. Each test configuration was performed in triplicate using independently prepared portions of homogenized material.

2.4. Magnetic Separation

Magnetic separation was carried out on the <3 mm fraction using a laboratory-scale plate-type magnetic separator equipped with a permanent magnet and electromagnets. The

technical specifications of the separator are provided in Table S4. The general configuration of the magnetic separator and the product collection system is shown in Scheme 3.

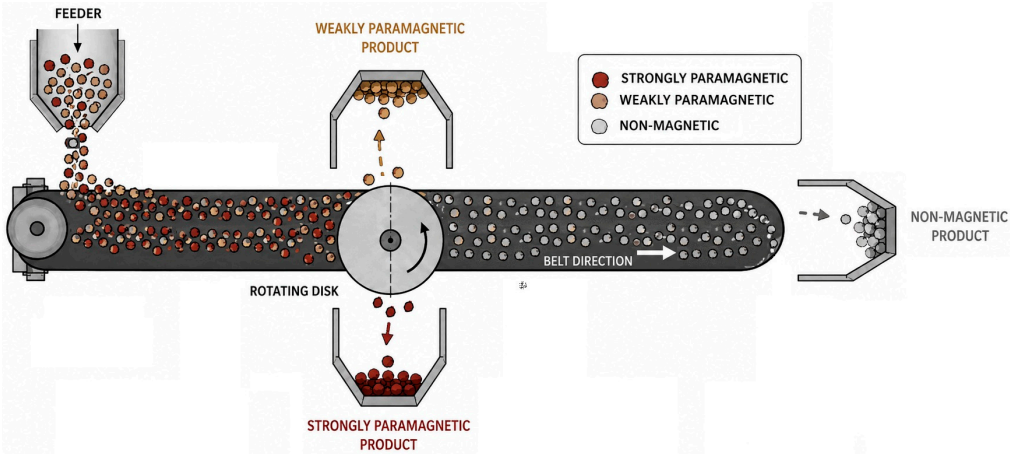

Scheme 3. Schematic representation of the laboratory-scale magnetic separator used in the study.

The feed material was introduced from the feeder onto the beginning of the conveyor belt and transported under a rotating magnetic disc. Depending on their magnetic susceptibility, particles were deflected from the belt trajectory to different collection zones. Strongly paramagnetic particles were deflected to the left and collected as the strongly paramagnetic product, whereas weakly paramagnetic particles were deflected to the right and collected as the weakly paramagnetic product. The remaining non-magnetic material continued along the belt and was discharged at the end of the conveyor into the non-magnetic product container. In some test configurations, the magnetically susceptible material was not divided into strongly and weakly paramagnetic products and was collected as a single paramagnetic product.

The feed masses used for magnetic separation are provided in Table S5. These masses were selected to obtain sufficient quantities of magnetically susceptible products for weighing and chemical analysis, while taking into account the availability of individual materials and their expected magnetic response.

Magnetic separation was conducted using the operating conditions provided in Table S6. The process was performed under different magnetic field intensity configurations to assess whether REE-bearing components showed preferential association with magnetically susceptible fractions. For most materials, three test configurations were applied. For Haldex K, the test was limited to one configuration because of the available material quantity and the very low yield of the magnetically susceptible product.

A constant feed rate and constant transport system velocities were maintained during the tests: feed rate of 8 g/min, belt speed of 0.6 m/s, and magnetic roll speed of 15 rpm. The non-magnetic fraction was determined from the mass balance of the feed and magnetically susceptible products. For product streams with a mass below 3 g, especially paramagnetic products, samples obtained under the same operating configuration were combined prior to chemical analysis in order to obtain sufficient analytical mass. The magnetic-separation products selected for chemical analysis and their corresponding sample codes are listed in Table S7.

2.5. Methodology for the Analysis of Selected Elements

In addition to the separation products, five feed samples representing the initial materials were prepared for chemical analysis: Paskov, Karviná, Haldex S, Haldex O, and Haldex K. The feed sample identification codes are provided in Table S8.

Chemical analyses were performed using inductively coupled plasma mass spectrometry (ICP–MS) at Bureau Veritas Commodities Canada Ltd. (Timmins, ON, Canada) Samples were prepared by fusion with a $LiBO_2/Li_2B_4O_7$ flux. The fused bead was dissolved in nitric acid, and the resulting solution was analyzed by ICP–MS to determine rare earth elements and selected accompanying elements. Loss on ignition (LOI) was determined by heating a representative portion of the sample and measuring the mass loss.

The analytical program was focused on bulk chemical composition and REE distribution between separation products, as determined by ICP–MS. Complementary mineralogical and magnetic characterization by SEM-EDS, XRD and VSM was not included in the present experimental scope. This was because the study was designed as a laboratory-scale process-response assessment of dry electrostatic and magnetic separation, rather than as a full mineralogical identification of REE host phases. Consequently, interpretations concerning REE-bearing phases, liberation behaviour and magnetic response are treated as indirect process-based indications derived from product chemistry, enrichment factors, product yield and mass distribution, rather than as direct mineralogical or magnetic confirmation.

2.6. Data Processing and Process Evaluation Indicators

2.6.1. Units, Notation, and Treatment of Values Below the Detection Limit

Concentrations of trace elements and rare earth elements were reported in ppm, equivalent to mg/kg. Major components and LOI were expressed in wt.%. Values reported by the laboratory as below the detection limit were treated as non-quantifiable values with only an upper boundary known. For calculations requiring numerical values, a substitute value equal to 0.5 × DL was applied. If a given element was reported as below the detection limit in both the feed and product, derived indicators for that element were not calculated.

2.6.2. Definitions of REE Sums

The total rare earth element content, ΣREE, was calculated as the sum of Sc, Y, and lanthanides from La to Lu:

$$\Sigma REE = Sc + Y + La + Ce + Pr + Nd + Sm + Eu + Gd + Tb + Dy + Ho + Er + Tm + Yb + Lu \quad (1)$$

The sum of light rare earth elements, ΣLREE, included lanthanides from La to Eu:

$$\Sigma LREE = La + Ce + Pr + Nd + Sm + Eu \quad (2)$$

The sum of heavy rare earth elements, ΣHREE, included Sc, Y, and lanthanides from Gd to Lu:

$$\Sigma HREE = Sc + Y + Gd + Tb + Dy + Ho + Er + Tm + Yb + Lu \quad (3)$$

The same definitions were applied consistently to feed materials and separation products.

2.6.3. Mass Yield and Mass Balance

The mass yield of a given product was calculated as

$$Y_i\ (\%) = m_i/m_F * 100 \quad (4)$$

where Y_i is the mass yield of product i, m_i is the mass of product i, and m_F is the mass of the feed.

The mass balance, also referred to as mass closure, was calculated as

$$MB(\%) = \Sigma m_i/m_F * 100 \quad (5)$$

where $\sum m_i$ is the sum of the masses of all collected products. Mass balance was used to assess the consistency of the separation tests and to identify possible losses related to dusting, particle carry-over, deposition on separator elements, transport, or auxiliary handling operations.

The masses of feeds and separation products were determined using a laboratory balance with a readability of ±0.01 g. Product yields and mass closures were calculated from the measured masses and then rounded for tabular presentation. For the purpose of laboratory-scale separation tests, mass closure within 99.5%–100.5% was treated as acceptable. Deviations within this range were interpreted as resulting mainly from weighing precision, rounding and minor handling effects rather than from systematic material loss. This criterion was particularly relevant for low-mass products, such as semi-conductive or paramagnetic fractions, where the relative influence of weighing uncertainty is higher.

2.6.4. Enrichment Factor (EF)

The enrichment factor, EF, was used to evaluate whether a given component was enriched or depleted in a product relative to the corresponding feed. It was calculated as

$$EF_{x,i} = C_{x,i}/C_{x,F} \quad (6)$$

where $EF_{x,i}$ is the enrichment factor of component x in product i, $C_{x,i}$ is the concentration of component x in product i, and $C_{x,F}$ is the concentration of component *x* in the feed.

An EF value greater than 1 indicates enrichment relative to the feed, whereas an EF value below 1 indicates depletion. EF values were calculated for ΣREE and selected individual REE.

2.6.5. Repeatability of Results: Standard Deviation and RSD

For product yields in each separation configuration, three independent replicate tests were performed. The repeatability of product yield was expressed using the standard deviation of yield, reported in percentage points. This parameter was used to describe the variability of product mass distribution between replicate tests.

Where parallel chemical determinations were available, the repeatability of ΣREE content was expressed using the relative standard deviation:

$$RSD(\%) = (SD/\bar{x}) \cdot 100 \quad (7)$$

where SD is the standard deviation of replicate measurements and $\bar{x}$ is the arithmetic mean. RSD was applied only to concentration data and not to product yield values.

2.6.6. Analytical Consistency Control: Sum of Major Components and LOI

To verify the consistency of the chemical data, a summary parameter was calculated as the sum of major components reported as oxides plus LOI. The obtained values were compared with 100% as an internal analytical consistency check, taking into account analytical uncertainty and rounding effects.

3. Results

3.1. Feed Characterization After Drying and Particle Size Preparation

The initial chemical composition of the feed materials prepared to the <3 mm particle size fraction is presented in Table 1. This fraction was used directly as the feed for magnetic separation and also constituted the starting material for further grinding to <45 μm prior to electrostatic separation.

Table 1. Initial chemical composition of feed materials in the <3 mm particle size fraction (rare earth elements determined by ICP–MS).

Feed Material	ΣREE (ppm)	Nd (ppm)	Pr (ppm)	Dy (ppm)	ΣLREE (ppm)	ΣHREE (ppm)	LOI (%)	Total Oxides + LOI (%)
Paskov	224.76	36.20	9.10	5.75	158.27	66.49	50.8	99.61
Karviná	209.81	30.89	8.26	4.59	151.37	58.44	18.5	99.84
Haldex S	222.69	32.40	8.68	5.28	157.91	64.78	26.3	99.83
Haldex O	250.54	37.00	9.92	5.63	181.11	69.43	33.9	99.73
Haldex K	109.33	16.90	4.31	2.83	77.12	32.21	12.5	99.84

The chemical composition presented in Table 1 refers to the <3 mm fraction. This fraction was used directly as the feed for magnetic separation and as the starting material for additional grinding prior to electrostatic separation. Therefore, the results in Table 1 provide the common reference composition for evaluating the response of the investigated materials to both dry separation methods.

The ΣREE content of the feed materials ranged from 109.33 ppm in Haldex K to 250.54 ppm in Haldex O. Paskov, Karviná, and Haldex S showed intermediate and relatively similar ΣREE contents, ranging from 209.81 to 224.76 ppm. In all feeds, ΣLREE exceeded ΣHREE, indicating the predominance of light rare earth elements in the analyzed materials.

Marked differences were observed in LOI, which ranged from 12.5% for Haldex K to 50.8% for Paskov. This variability indicates substantial differences in the proportion of organic and/or volatile components between the investigated waste streams. The sum of major oxides and LOI remained close to 100% for all feed samples, confirming the internal consistency of the chemical data.

Because the electrostatic separation feed was additionally ground to <45 μm, EF values for electrostatic products were calculated using the corresponding <3 mm feed composition as the reference. This approach provides a consistent basis for comparing the five materials, although it does not define the liberation size of REE-bearing phases.

3.2. Electrostatic Separation: Product Yields and Mass Balance

As a result of electrostatic separation, each feed material prepared to the <45 μm particle size fraction was divided into three streams: conductive, semi-conductive, and non-conductive products. The mass distribution for Test I and Test II is presented in Table 2, including the mass of obtained products, their corresponding percentage yields relative to the feed mass, and the standard deviation of the yields.

Table 2. Mass distribution in the electrostatic separation process (products: conductive, semi-conductive, and non-conductive).

Sample	Test	Feed Mass (g)	Conductive Product, g/%/SD, Percentage Points	Semi-Conductive Product, g/%/SD, Percentage Points	Non-Conductive Product, g/%/SD, Percentage Points	Mass Closure (%)
Paskov	I	250	189.8/75.9/0.8	25.2/10.1/0.4	35.0/14.0/0.6	100.0
	II	300	208.5/69.5/0.9	6.3/2.1/0.2	85.2/28.4/0.7	100.0
Karviná	I	200	128.0/64.0/1.0	3.6/1.8/0.2	68.4/34.2/0.8	100.0
	II	300	247.8/82.6/0.7	6.1/2.0/0.2	46.8/15.6/0.5	100.2
Haldex S	I	150	114.0/76.0/0.9	6.0/4.0/0.3	30.0/20.0/0.6	100.0
	II	1350	1201.5/89.0/0.5	118.8/8.8/0.4	29.7/2.2/0.2	100.0
Haldex O	I	250	215.5/86.2/0.6	14.5/5.8/0.3	20.0/8.0/0.4	100.0
	II	250	185.3/74.1/0.8	44.5/17.8/0.6	20.2/8.1/0.3	100.0
Haldex K	I	100	35.2/35.2/0.7	11.1/11.1/0.4	53.7/53.7/1.0	100.0
	II	100	60.5/60.5/0.8	7.8/7.8/0.3	31.7/31.7/0.9	100.0

Mass-closure values were calculated from measured product masses and rounded for tabular presentation. Values close to 100% do not imply complete absence of particle losses but indicate that possible losses were within the uncertainty and rounding range of the laboratory mass-balance procedure.

The mass yield distribution shown in Figure 4 confirms that the conductive product dominated in most electrostatic-separation tests, whereas Haldex K showed a different response, with a high share of the non-conductive product in Test I.

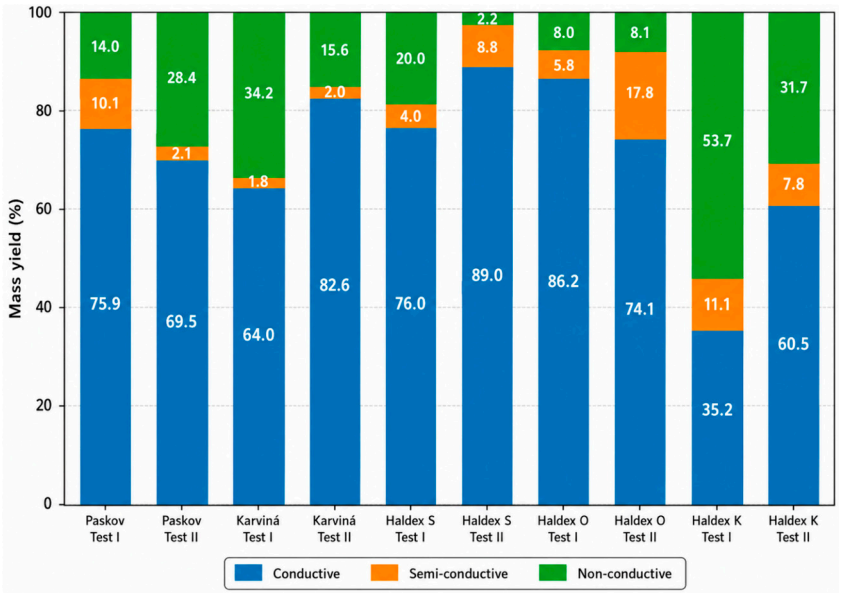

Figure 4. Mass yield distribution of electrostatic-separation products obtained for the investigated post-mining waste materials under Test I and Test II conditions. The stacked bars show the relative shares of conductive, semi-conductive and non-conductive products, highlighting the variability in product distribution between materials and operating conditions.

For most materials, electrostatic separation produced a dominant conductive fraction. This was particularly evident for Paskov, Karviná, Haldex S, and Haldex O, where the conductive product generally accounted for more than 60% of the feed mass. The semi-conductive fraction was usually minor, whereas the non-conductive product varied more strongly between materials and test conditions.

Haldex K showed a different mass distribution pattern. In Test I, the non-conductive product was the dominant stream, accounting for 53.7% of the feed mass, whereas in Test II the conductive product increased to 60.5%. This result confirmed that Haldex K responded differently to electrostatic separation than the other investigated materials.

The standard deviations of product yields ranged from 0.2 to 1.0 percentage points, indicating good repeatability of the mass distribution under the applied operating conditions. Mass closure ranged from 100.0% to 100.2%, which was within the adopted acceptable closure range of 99.5%–100.5%. The highest value, 100.2%, was obtained for Karviná Test II. This slight positive deviation was attributed to weighing precision and rounding of product masses and yields in the table, rather than to a systematic measurement artefact. This is particularly relevant for low-mass products, such as the semi-conductive fraction, where small absolute differences in measured mass may have a proportionally larger effect. Overall, the mass balance results indicate adequate mass-accounting consistency under the applied laboratory conditions. This should not be interpreted as complete absence of fine-particle escape, local deposition or handling losses, but rather as evidence that such effects were not large enough to materially affect the calculated product-yield distribution.

3.3. Electrostatic Separation: Chemical Composition of Products and REE Enrichment Factors

3.3.1. Results of Electrostatic Separation—ΣREE and Selected Rare Earth Elements

The full chemical composition of electrostatic-separation products is provided in Table S9. This supplementary table includes ΣREE, selected REE, ΣLREE, ΣHREE, LOI, and the oxide balance for conductive, semi-conductive, and non-conductive products obtained under Test I and Test II. In the main text, the interpretation focuses on the main concentration ranges and material-dependent trends, while the enrichment factors and EF–yield relationships are discussed in the following subsection.

Electrostatic separation produced a mass distribution dominated mainly by the conductive fraction in most tested materials, whereas Haldex K showed a distinct response, with a high share of the non-conductive product in Test I.

The ΣREE contents of electrostatic-separation products generally remained close to the corresponding feed values, indicating limited changes in total REE concentration during electrostatic separation. For Paskov, the highest ΣREE content was observed in the non-conductive product from Test II, reaching 245.38 ppm. For Karviná and Haldex O, the product compositions remained close to the corresponding feed compositions, which indicates weak redistribution of REE between conductive, semi-conductive and non-conductive fractions.

Haldex S showed a wider range of ΣREE contents, from 182.74 to 228.38 ppm, with the lowest value observed in the non-conductive product from Test II. In contrast, Haldex K showed the widest relative variation among products, with ΣREE ranging from 76.31 ppm in the non-conductive product from Test I to 137.85 ppm in the conductive product from Test II.

LOI values varied substantially between materials and products. Particularly high LOI values were observed for Haldex K products, ranging from 77.2% to 88.6%. This finding confirmed that Haldex K differed strongly from the other materials in terms of organic- and/or volatile-rich components after fine grinding and electrostatic separation. The oxide balance including LOI remained close to 100% for all electrostatic products, confirming the analytical consistency of the results.

Differences in LOI between the <3 mm feed materials and the <45 µm electrostatic products should be interpreted with caution. They may reflect particle-size-related heterogeneity and redistribution of organic- or volatile-rich components during sample preparation and separation, rather than direct removal of these components by electrostatic separation.

3.3.2. Enrichment Factors for ΣREE and Selected Rare Earth Elements in Electrostatic-Separation Products

The enrichment factor was used to compare REE redistribution between electrostatic-separation products. Table 3 presents EF values for ΣREE and selected REE in conductive, semi-conductive, and non-conductive products obtained under Test I and Test II.

The graphical comparison of EF ΣREE values for electrostatic-separation products is presented in Figure 5. Most products showed EF values close to unity, indicating limited ΣREE redistribution, while the highest enrichment was observed for the Haldex K conductive product obtained under Test II conditions.

Electrostatic separation resulted mainly in EF values close to unity, indicating limited ΣREE enrichment. For Paskov, the highest EF ΣREE was obtained in the non-conductive product from Test II (1.09). This product also showed stronger enrichment of Nd and Pr, both reaching EF = 1.33, while EF Dy reached 1.14.

Table 3. Enrichment factors for ΣREE and selected rare earth elements in electrostatic-separation products relative to the corresponding feeds (dimensionless values).

Material	Test	Product	EF ΣREE	EF Nd	EF Pr	EF Dy
Paskov	Test I	Conductive	0.99	0.94	0.97	0.92
	Test I	Semi-conductive	**1.05**	**1.07**	**1.04**	**1.05**
	Test I	Non-conductive	1.00	**1.01**	1.00	**1.01**
Paskov	Test II	Conductive	0.99	0.93	0.97	0.93
	Test II	Semi-conductive	**1.06**	**1.17**	**1.15**	**1.07**
	Test II	Non-conductive	**1.09**	**1.33**	**1.33**	**1.14**
Karviná	Test I	Conductive	1.00	**1.01**	**1.02**	0.99
	Test I	Semi-conductive	**1.05**	**1.11**	**1.07**	**1.09**
	Test I	Non-conductive	1.00	0.99	0.99	1.00
Karviná	Test II	Conductive	**1.05**	**1.05**	**1.05**	**1.04**
	Test II	Semi-conductive	**1.01**	**1.02**	**1.01**	**1.07**
	Test II	Non-conductive	**1.03**	**1.05**	**1.05**	**1.05**
Haldex S	Test I	Conductive	0.97	0.99	0.96	**1.06**
	Test I	Semi-conductive	**1.03**	**1.07**	**1.05**	**1.08**
	Test I	Non-conductive	0.96	1.00	0.96	**1.04**
Haldex S	Test II	Conductive	**1.02**	**1.04**	0.97	**1.60**
	Test II	Semi-conductive	0.90	0.94	0.91	0.97
	Test II	Non-conductive	0.82	0.85	0.81	0.93
Haldex O	Test I	Conductive	1.00	**1.01**	1.00	1.00
	Test I	Semi-conductive	0.96	0.94	0.96	0.98
	Test I	Non-conductive	**1.02**	**1.02**	**1.02**	**1.04**
Haldex O	Test II	Conductive	0.97	0.96	0.97	0.97
	Test II	Semi-conductive	0.97	0.96	0.97	0.99
	Test II	Non-conductive	0.99	0.99	0.99	**1.01**
Haldex K	Test I	Conductive	**1.07**	**1.06**	**1.06**	**1.11**
	Test I	Semi-conductive	0.82	0.87	0.86	0.86
	Test I	Non-conductive	0.70	0.72	0.71	0.73
Haldex K	Test II	Conductive	**1.26**	**1.30**	**1.31**	**1.30**
	Test II	Semi-conductive	0.88	0.91	0.92	0.90
	Test II	Non-conductive	0.79	0.81	0.79	0.88

For Karviná and Haldex O, EF values remained close to unity across most products, indicating weak or negligible concentration effects. Haldex S showed selective enrichment of Dy in the conductive product from Test II, where EF Dy reached 1.60, although EF ΣREE remained close to unity.

The clearest enrichment pattern was observed for Haldex K. The conductive product from Test II showed simultaneous enrichment of ΣREE, Nd, Pr, and Dy, with EF values of 1.26, 1.30, 1.31, and 1.30, respectively. This was the most consistent electrostatic separation response among the investigated materials.

The selective enrichment patterns for the two most promising electrostatic-separation products are compared in Figure 6, namely the Paskov Test II non-conductive product and the Haldex K Test II conductive product.

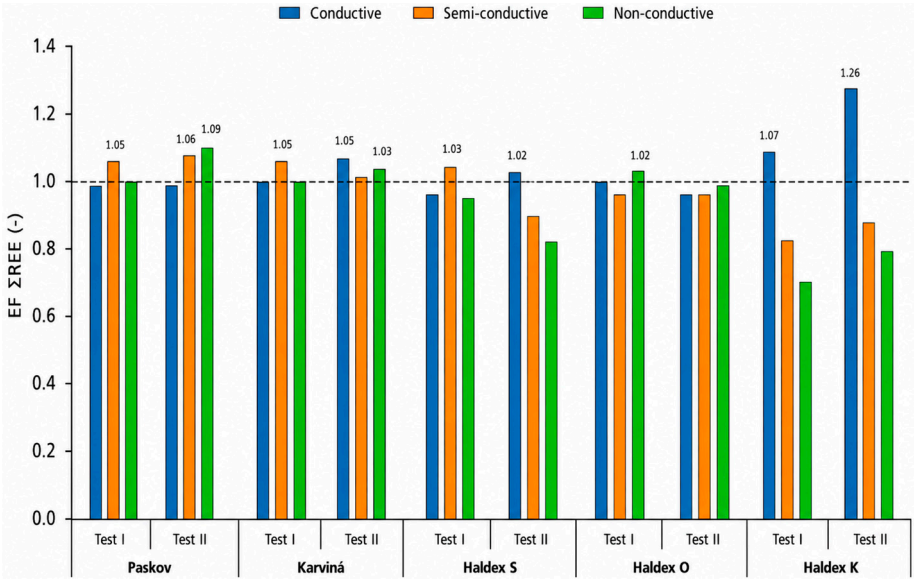

Figure 5. Enrichment factor (EF) of ΣREE in electrostatic-separation products relative to the corresponding feed materials. The results are shown for conductive, semi-conductive and non-conductive products obtained under Test I and Test II conditions. The dashed horizontal line at EF = 1 indicates no enrichment relative to the feed; values above this line indicate enrichment, whereas values below it indicate depletion.

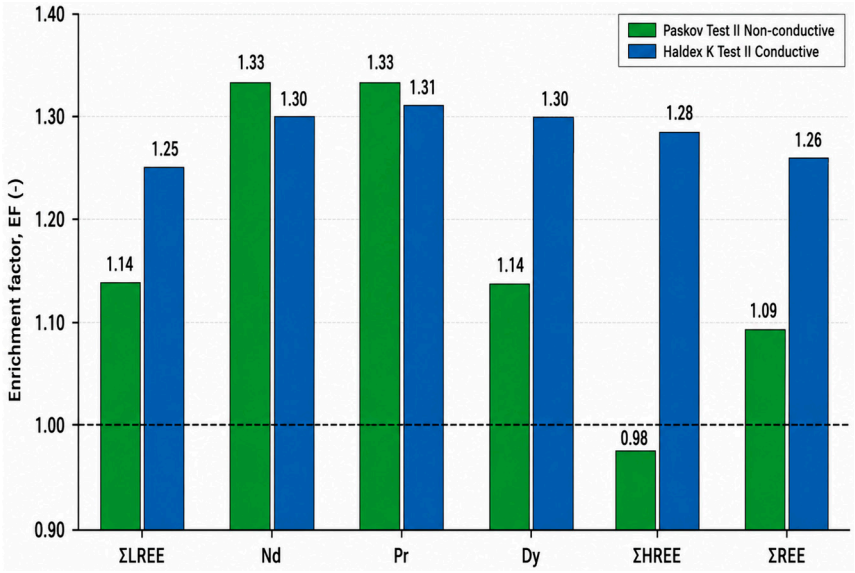

Figure 6. Selective enrichment pattern for the most promising electrostatic-separation products, comparing the Paskov Test II non-conductive product and the Haldex K Test II conductive product in terms of EF values for ΣLREE, Nd, Pr, Dy, ΣHREE, and ΣREE. The dashed horizontal line at EF = 1 indicates no enrichment relative to the corresponding feed.

Figure 6 shows that the Paskov Test II non-conductive product was characterized mainly by selective enrichment of Nd and Pr, whereas the Haldex K Test II conductive product exhibited a more balanced enrichment pattern across both light and heavy REE indicators. In particular, Haldex K Test II showed higher EF values for ΣREE, ΣLREE and ΣHREE, confirming that this product represented the most consistent electrostatic-separation response among the investigated materials.

The relationship between EF ΣREE and product yield for electrostatic-separation products is shown in Figure 7.

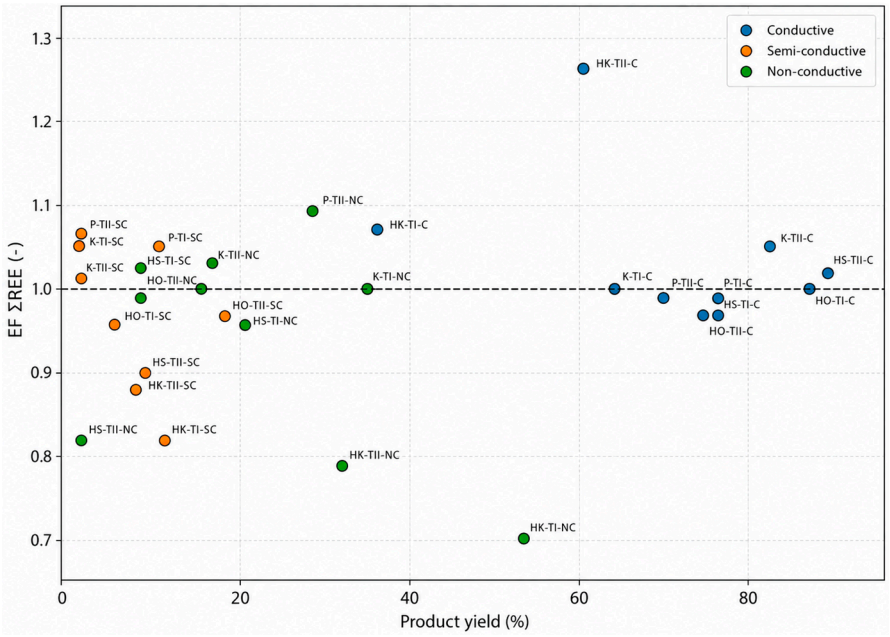

Figure 7. EF ΣREE as a function of product yield for electrostatic-separation products.

Figure 7 shows that electrostatic-separation products with EF ΣREE values above unity were observed only in selected cases. The most favourable response was obtained for the Haldex K conductive product from Test II, although the enrichment remained moderate. This indicates that electrostatic separation produced limited and material-specific REE redistribution rather than a clearly efficient concentration effect.

3.4. Magnetic Separation: Product Yields Under Sequentially Varying Magnetic Field Intensity

The mass distribution obtained during magnetic separation of the <3 mm fraction, including magnetically susceptible products and the non-magnetic product, is presented in Table 4. In Test III, the magnetically susceptible stream was additionally divided into strongly and weakly paramagnetic fractions.

Table 4. Mass distribution in the magnetic separation process (magnetically susceptible and non-magnetic products). * none—the fraction was not separated in Tests I and II; ** none—the combined paramagnetic product was not collected in Test III because the magnetically susceptible stream was divided into strongly and weakly paramagnetic fractions.

Sample	Test	Feed Mass (g)	Paramagnetic Product, g/%/SD, Percentage Points	Strongly Paramagnetic Product, g/%/SD, Percentage Points	Weakly Paramagnetic Product, g/%/SD, Percentage Points	Non-Magnetic Product, g/%/SD, Percentage Points
Paskov	I	300	5.1/1.7/0.10	* none	* none	294.9/98.3/0.07
	II	50	5.5/11.0/0.30	* none	* none	44.5/89.0/0.20
	III	350	** none	5.7/1.6/0.08	7.4/2.1/0.10	336.9/96.3/0.09
Karviná	I	550	5.1/0.9/0.05	* none	* none	544.9/99.1/0.04
	II	450	5.7/1.3/0.07	* none	* none	444.3/98.7/0.04
	III	950	** none	6.2/0.7/0.04	3.9/0.3/0.03	939.9/98.9/0.03
Haldex S	I	1700	6.5/0.4/0.03	* none	* none	1693.5/99.6/0.02
	II	850	5.5/0.6/0.04	* none	* none	844.5/99.4/0.04
	III	1450	** none	14.2/1.0/0.08	5.6/0.4/0.04	1430.2/98.6/0.06
Haldex O	I	650	5.9/0.9/0.06	* none	* none	644.1/99.1/0.05
	II	450	10.9/2.4/0.15	* none	* none	439.1/97.6/0.10
	III	550	** none	6.8/1.2/0.07	8.5/1.5/0.09	534.7/97.2/0.09
Haldex K	I	2450	5.2/0.2/0.02	* none	* none	2444.8/99.8/0.03

The mass-yield distribution of magnetic-separation products is shown in Figure 8. The figure illustrates the dominant contribution of the non-magnetic fraction in all test configurations and the very limited mass recovery of magnetically susceptible products.

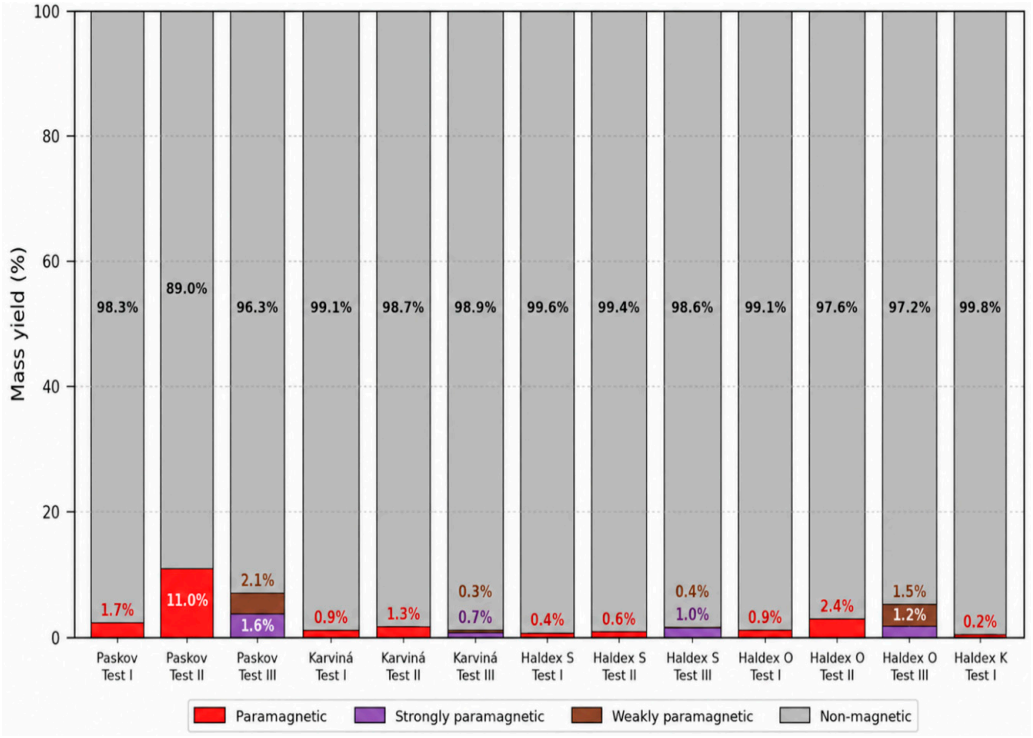

Figure 8. Mass yield distribution of magnetic-separation products obtained from the investigated post-mining waste materials. The stacked bars show the relative shares of paramagnetic, strongly paramagnetic, weakly paramagnetic and non-magnetic products obtained under the applied magnetic-separation conditions.

Overall, magnetic separation produced a mass distribution strongly dominated by the non-magnetic fraction. In most configurations, magnetically susceptible products represented only a small proportion of the feed mass, generally below 2.5%. In Haldex K, the paramagnetic product accounted for only 0.2% of the feed mass, while the non-magnetic fraction represented 99.8%.

The mass balance remained consistent across all magnetic-separation tests. The non-magnetic fraction was calculated from the feed mass and the collected magnetically susceptible products, which allowed possible handling or separation losses to be reflected in the mass-closure assessment. The calculated product yields corresponded to the feed mass within rounding accuracy, indicating that particle losses during magnetic separation were limited.

3.5. Magnetic Separation: Chemical Composition of Products and REE Enrichment Factors

The full chemical composition of magnetically susceptible products is provided in Table S10, while the corresponding EF values for ΣREE and selected REE are given in Table 5. These results were used to assess whether REE-bearing components preferentially reported to magnetically susceptible fractions and whether any observed chemical enrichment was relevant when interpreted together with product yield.

Table 5. Enrichment factors for ΣREE and selected rare earth elements in magnetic-separation products relative to the corresponding feeds (dimensionless values).

Feed Material	Test	Product	EF ΣREE	EF Nd	EF Pr	EF Dy
Paskov	I	Paramagnetic	0.92	0.89	0.82	**1.32**
	II	Paramagnetic	**1.05**	**1.05**	1.00	**1.38**
	III	Strongly paramagnetic	0.91	0.81	0.76	**1.31**
	III	Weakly paramagnetic	**1.12**	**1.07**	**1.07**	**1.28**
Karviná	I	Paramagnetic	0.65	0.72	0.64	**1.01**
	II	Paramagnetic	0.70	0.74	0.65	**1.05**
	III	Strongly paramagnetic	0.58	0.59	0.52	0.90
	III	Weakly paramagnetic	0.68	0.68	0.64	**1.04**
Haldex S	I	Paramagnetic	0.72	0.91	0.73	1.00
	II	Paramagnetic	0.80	0.82	0.77	**1.09**
	III	Strongly paramagnetic	0.73	0.70	0.62	**1.12**
	III	Weakly paramagnetic	0.90	0.94	0.87	**1.31**
Haldex O	I	Paramagnetic	0.57	0.58	0.56	0.76
	II	Paramagnetic	0.79	0.79	0.78	0.90
	III	Strongly paramagnetic	0.64	0.62	0.60	0.79
	III	Weakly paramagnetic	0.91	0.91	0.90	0.99
Haldex K	I	Paramagnetic	**1.30**	**1.35**	**1.28**	**1.76**

3.5.1. ΣREE, Selected REE, LOI, and Oxide Balance

The full dataset for magnetically susceptible products, including ΣREE, selected REE, ΣLREE, ΣHREE, LOI and oxide balance, is provided in Table S10. In the main text, the interpretation focuses on the main concentration trends and on their relationship with the very low mass yields of magnetic products.

For most materials, the magnetically susceptible products had lower ΣREE contents than the corresponding feeds. This effect was particularly clear for Karviná, where ΣREE in the magnetic products ranged from 120.83 to 146.71 ppm, compared with 209.81 ppm in the feed. Similar depletion was observed for Haldex S and Haldex O, although the magnitude varied between test conditions.

Paskov showed a less uniform response. Most magnetic products had ΣREE contents close to or below the feed value, but the weakly paramagnetic product from Test III reached 251.29 ppm, exceeding the feed concentration. Haldex K showed the strongest increase in ΣREE concentration among the magnetic products, with 141.77 ppm in the paramagnetic product compared with 109.33 ppm in the feed.

Despite these selected increases in concentration, the mass yields of magnetically susceptible products were generally low, particularly for Haldex K. Therefore, the chemical enrichment observed in individual magnetic products should be interpreted together with the corresponding product yields. This is especially important for the Haldex K paramagnetic product, where the increase in ΣREE concentration was accompanied by a very low product yield, limiting its practical significance as a pre-concentration product.

LOI values in magnetic products varied between materials, with the highest value observed for Haldex K. The total oxide balance including LOI remained close to 100%, confirming the analytical consistency of the data. However, no consistent LOI–ΣREE relationship was observed for magnetic products, indicating that LOI alone cannot be used as a predictor of REE concentration in magnetically susceptible fractions.

3.5.2. Enrichment Factors for ΣREE and Selected Rare Earth Elements in Magnetic-Separation Products

Table 5 presents the EF values for ΣREE and selected REE in magnetic-separation products. These values complement the mass distribution data and indicate whether the magnetically susceptible fractions were enriched or depleted relative to the corresponding feed materials.

The graphical comparison of EF ΣREE values for magnetic-separation products is presented in Figure 9. Most magnetically susceptible products showed EF values below unity, indicating ΣREE depletion relative to the feed, while enrichment was observed only in selected cases, particularly for the Haldex K paramagnetic product.

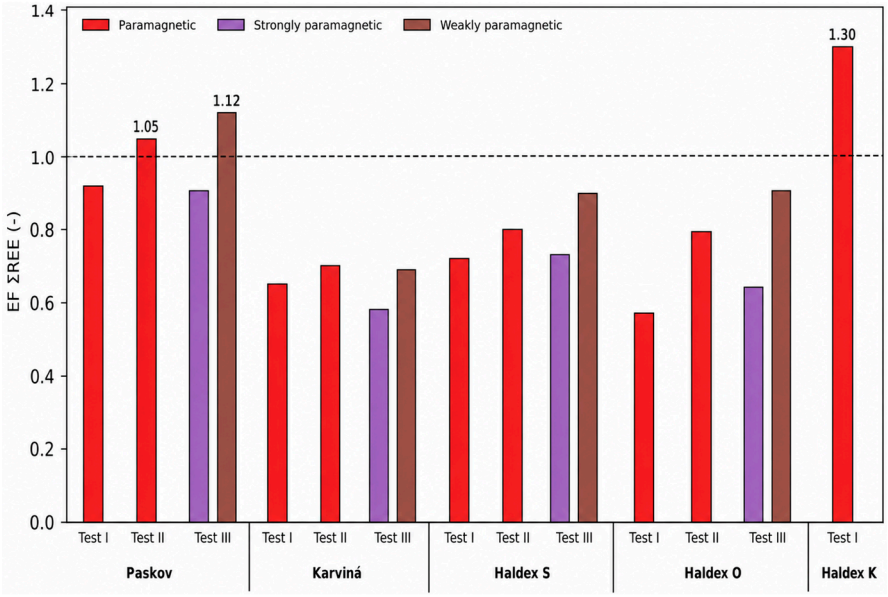

Figure 9. Enrichment factor (EF) of ΣREE in magnetically susceptible products relative to the corresponding feed materials. The results are shown for paramagnetic, strongly paramagnetic and weakly paramagnetic products obtained during magnetic separation. The dashed horizontal line at EF = 1 indicates no enrichment relative to the feed; values above this line indicate enrichment, whereas values below it indicate depletion.

For most materials, EF ΣREE values in magnetic products were below 1, indicating depletion relative to the feed. The strongest depletion was observed for Karviná, where EF ΣREE ranged from 0.58 to 0.70.

Limited enrichment was observed only in selected cases. For Paskov, EF ΣREE reached 1.05 in the paramagnetic product from Test II and 1.12 in the weakly paramagnetic product from Test III. For Haldex S, EF ΣREE remained below 1, although selective enrichment of Dy was observed in the weakly paramagnetic product from Test III.

The highest EF values in magnetic separation were obtained for Haldex K. The paramagnetic product reached EF ΣREE = 1.30, with EF Dy = 1.76. However, this product represented only 0.2% of the feed mass, which strongly limits the practical significance of this enrichment.

The relationship between EF ΣREE and product yield for magnetic-separation products is shown in Figure 10.

Figure 10 shows that magnetic separation did not produce a favourable combination of high EF ΣREE and high product yield. Most magnetically susceptible products were characterized by low yields and EF ΣREE values below or close to unity. Although the Haldex K paramagnetic product showed the highest EF ΣREE value of 1.30, its yield was only 0.2%, which strongly limits its practical relevance as a pre-concentration product.

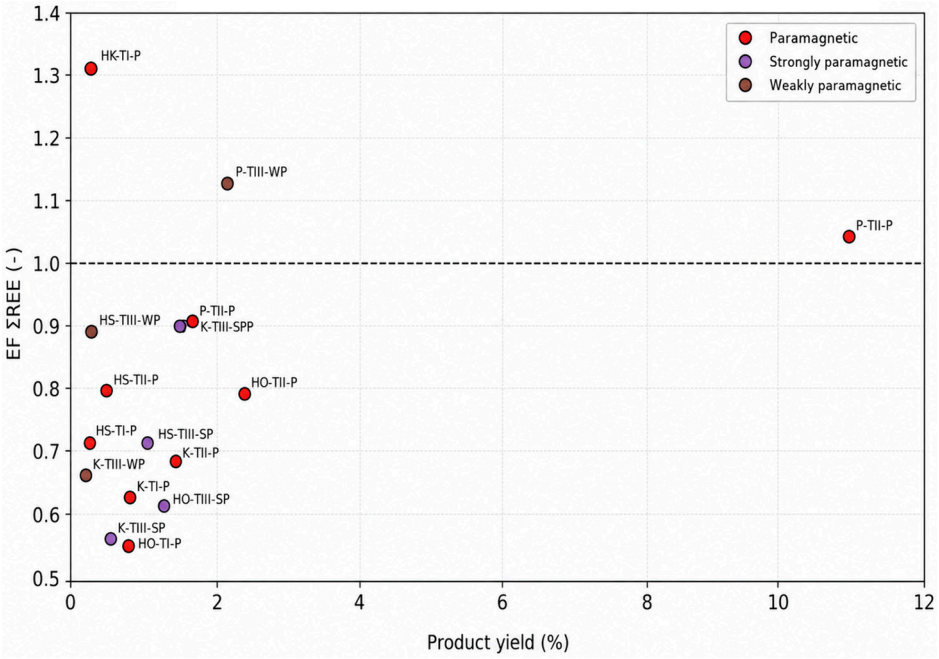

Figure 10. EF ΣREE as a function of product yield for magnetic-separation products. The figure compares the enrichment factor of ΣREE with the corresponding mass yield of paramagnetic, strongly paramagnetic and weakly paramagnetic products. The dashed horizontal line at EF = 1 indicates no enrichment relative to the feed, whereas values above this line indicate enrichment.

The only product combining a relatively high yield with EF ΣREE above unity was the Paskov Test II paramagnetic product, with EF ΣREE = 1.05 and a yield of 11.0%. However, this enrichment was very weak and does not indicate effective REE beneficiation. Therefore, the EF–yield relationship confirms that magnetic separation mainly provided diagnostic information on REE partitioning rather than a practically useful concentration effect.

3.6. Relationship Between LOI and ΣREE in Feed and Separation Products

The relationship between LOI and ΣREE (Figures 11 and 12) was analyzed to assess whether variations in organic and/or volatile matter content were accompanied by systematic changes in total REE content. Because electrostatic and magnetic separation were performed on different particle-size fractions and produced different product categories, the LOI–ΣREE relationship is presented separately for electrostatic and magnetic-separation products.

Figure 11 shows that no simple positive relationship between LOI and ΣREE can be identified for the feed materials and electrostatic-separation products. Most Paskov, Karviná, Haldex S and Haldex O products remained within a relatively narrow ΣREE range, despite differences in LOI. In contrast, Haldex K products formed a distinct high-LOI cluster, with LOI values above 77% and relatively low to moderate ΣREE contents. This confirms that the different behaviour of Haldex K was associated with a markedly different material response, but LOI alone cannot explain REE enrichment or depletion. The comparison should also be interpreted with caution because the feed composition refers to the <3 mm fraction, whereas electrostatic separation was performed on the additionally ground <45 μm fraction.

Figure 12 also indicates the absence of a consistent LOI–ΣREE trend for magnetic-separation products. Some weakly paramagnetic products showed relatively high ΣREE contents, but this was not consistently associated with high LOI. Conversely, the Haldex K paramagnetic product showed elevated LOI compared with most magnetic products, but its ΣREE content remained moderate. These results suggest that LOI reflects material

heterogeneity and the redistribution of organic- or volatile-rich components, but it is not a standalone predictor of REE concentration in the separated products.

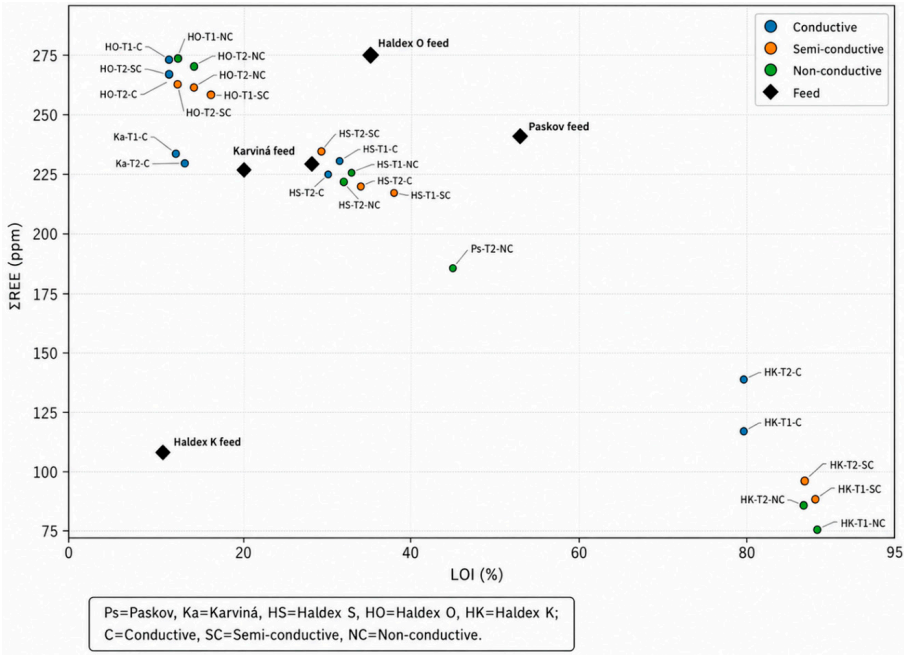

Figure 11. Relationship between LOI and ΣREE content for feed materials and electrostatic-separation products.

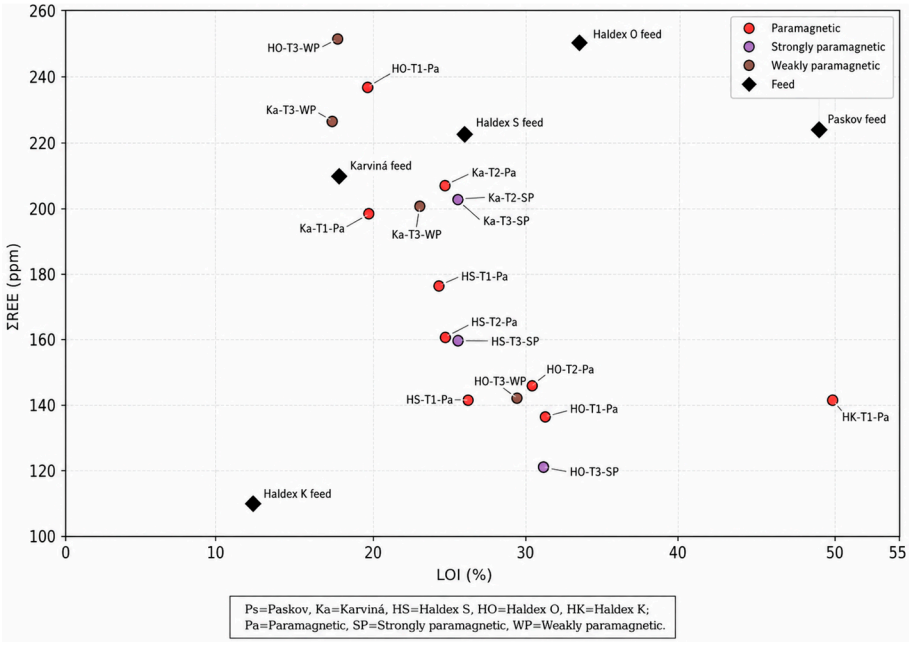

Figure 12. Relationship between LOI and ΣREE content for feed materials and magnetic-separation products.

3.7. Repeatability of Results in Parallel Tests and Sensitivity to Operating Parameters

The repeatability of product yields was assessed using the standard deviation calculated from three replicate tests. For electrostatic separation, the standard deviation ranged from 0.2 to 1.0 percentage points, indicating stable product mass distribution under the applied operating conditions.

For magnetic separation, the standard deviation of product yields ranged from 0.02 to 0.30 percentage points. The highest variability was observed for the Paskov Test II

configuration, which was conducted with the lowest feed mass. In the remaining configurations, variability was lower, despite the very small absolute masses of magnetically susceptible products.

Where replicate chemical determinations were available, the repeatability of ΣREE concentration was evaluated using RSD. The RSD values ranged from approximately 1.5% to 4.8%, with higher values observed for low-mass magnetic products and Haldex K-derived products. These values indicate acceptable analytical repeatability for the purpose of comparing feed and product compositions.

A summary of product-yield repeatability and ΣREE repeatability is presented in Table 6.

Table 6. Repeatability of product yields and ΣREE content where replicate chemical determinations were available.

Separation Process	Product Type	Yield Range (%)	SD of Yield, Percentage Points (Min–Max)	RSD ΣREE (%) (Min–Max)
Electrostatic	Conductive product	35.2–89.0	0.5–1.0	1.5–4.2
	Semi-conductive product	1.8–17.8	0.2–0.6	1.8–4.5
	Non-conductive product	2.2–53.7	0.2–1.0	1.6–4.8
Magnetic	Paramagnetic product (combined)	0.2–11.0	0.02–0.30	2.0–4.8
	Strongly paramagnetic product	0.7–1.6	0.04–0.08	1.8–4.5
	Weakly paramagnetic product	0.3–2.1	0.03–0.10	1.7–4.6

Overall, the Results section shows that electrostatic separation produced only moderate and material-specific REE enrichment, whereas magnetic separation was characterized by very low yields of magnetically susceptible products and frequent depletion of ΣREE in these products. The EF–yield relationships presented in Figures 7 and 10 confirm that products with EF ΣREE values above unity were observed only in selected cases and were generally moderate or associated with low product yields. The LOI–ΣREE relationships presented in Figures 11 and 12 further indicate that LOI alone does not explain the observed REE redistribution. Therefore, EF values and ΣREE contents should be interpreted together with product yield, mass distribution and material-specific characteristics. These results provide the basis for further discussion of the limited practical beneficiation effect and the diagnostic value of the applied dry separation methods.

4. Discussion

4.1. Experimental Comparability and Controlled-Variable Limitations

The results should be interpreted as a comparative assessment of material response under predefined laboratory conditions. The purpose was to compare five heterogeneous coal-derived post-mining waste streams in terms of product yield, mass distribution, enrichment factor, LOI and EF–yield relationships, rather than to optimize separator performance for each individual material.

The <3 mm and <45 µm fractions were used as operational feed-size classes suitable for the applied magnetic and electrostatic separators, respectively. They should not be interpreted as experimentally confirmed liberation sizes of REE-bearing phases. Because SEM–EDS, XRD and VSM analyses were outside the present experimental scope, interpretations concerning REE hosts, liberation behaviour and magnetic response remain indirect and are based on product chemistry and separation response.

4.2. Material-Dependent Electrostatic Separation Response

Electrostatic separation produced moderate and material-specific enrichment effects. In most products, EF ΣREE values remained close to unity, indicating that the separated fractions retained a chemical composition similar to that of the corresponding feed. This suggests that, under the applied laboratory conditions, REE-bearing components were not strongly partitioned according to electrical conductivity, charge retention or dielectric response.

This behaviour is consistent with the general principles of electrostatic and triboelectric separation, where separation efficiency depends on several interacting factors, including particle size, surface condition, moisture content, contact charging behaviour, mineralogical composition and separator configuration. In the present study, the applied electrode voltage and drum operating conditions produced measurable changes in mass distribution, but these changes were not generally accompanied by strong ΣREE enrichment.

Selected products nevertheless showed evidence of preferential REE partitioning. The clearest response was observed for Haldex K, where the conductive product from Test II reached EF ΣREE = 1.26 and showed simultaneous enrichment of Nd, Pr and Dy. A weaker but still visible effect was observed for the Paskov non-conductive product from Test II, particularly for Nd and Pr. These cases indicate that electrostatic separation can reveal material-dependent differences in REE partitioning, even when the overall enrichment effect remains limited.

The behaviour of Haldex K differed from that of the other materials. Although this material had the lowest ΣREE content in the feed, it showed the most distinct electrostatic enrichment pattern and high LOI values in several electrostatic products. This suggests that its separation response may have been influenced by a different distribution of organic-rich, carbonaceous or fine mineral components. The LOI–ΣREE relationship supports this interpretation, as Haldex K electrostatic products formed a distinct high-LOI cluster, whereas no general LOI–ΣREE correlation was observed across all materials and products.

Several possible REE associations may be inferred from the chemical composition and from literature data for coal-derived materials. REE may occur in fine-grained aluminosilicate phases, accessory phosphate or silicate minerals, heavy minerals, Fe-bearing phases, or surface-bound components associated with clay minerals and organic-rich particles. In the case of Haldex K, the high LOI and distinct electrostatic response suggest that carbonaceous or organic-rich particles may have affected the electrical behaviour of the material and the partitioning of REE-bearing components. However, this interpretation requires mineralogical verification because SEM–EDS and XRD analyses were not included in the present experimental scope.

Overall, electrostatic separation provided useful information on material-specific separability, but the magnitude of enrichment was limited. Its main relevance in this study is the identification of selected material-dependent partitioning effects and the assessment of whether further downstream extraction studies may be justified for specific separated products.

4.3. Limited Magnetic Separation Response and Role of Magnetic Susceptibility

Magnetic separation showed a more limited enrichment response than electrostatic separation. The main constraint was the combination of very low yields of magnetically susceptible products and frequent depletion of ΣREE in these products. In most configurations, the non-magnetic fraction dominated the mass balance, whereas the paramagnetic, strongly paramagnetic and weakly paramagnetic products represented only a small proportion of the feed. Moreover, EF ΣREE values in magnetic products were commonly below unity, especially for Karviná, Haldex S and Haldex O.

These results indicate that REE-bearing components were generally not preferentially associated with phases of increased magnetic susceptibility under the applied separation conditions. Several factors may explain this behaviour. First, REE in coal-derived waste may occur as finely dispersed phases or as inclusions within aluminosilicate particles, which do not necessarily respond to magnetic separation. Second, if REE are hosted by non-magnetic or only weakly magnetic mineral phases, their recovery into magnetically susceptible products will be inherently limited. Third, the <3 mm fraction used for magnetic separation was an operational feed-size class, not an experimentally confirmed liberation size. Composite particles may therefore have reduced separation selectivity.

The magnetic separation results are consistent with the interpretation that dry magnetic separation primarily affected magnetically susceptible mineral components, while REE redistribution depended on whether REE-bearing phases were physically or mineralogically associated with those components. If such association is weak or absent, magnetic separation may concentrate or remove Fe-bearing particles without producing meaningful ΣREE enrichment. Because VSM measurements were not performed, the magnetic response of the feeds and products could not be independently quantified; therefore, the interpretation is based on product yield, chemical redistribution and EF values.

The Haldex K paramagnetic product illustrates the importance of interpreting EF values together with product yield. This product reached EF ΣREE = 1.30 and EF Dy = 1.76, indicating that a small fraction of the material may have contained REE associated with magnetically susceptible components. However, the mass yield of this product was only 0.2% of the feed. From a process perspective, such a low yield strongly limits the relevance of this enrichment unless subsequent extraction tests demonstrate a clear advantage for this fraction.

Overall, magnetic separation provided mainly diagnostic information on REE partitioning in the investigated materials. The results show that, for most of the analyzed coal-derived post-mining waste streams, REE-bearing components were not sufficiently associated with magnetically susceptible fractions to generate a favourable EF–yield relationship. This finding is important for process-route selection because it indicates limited potential for mass reduction by magnetic separation prior to downstream REE extraction.

4.4. Implications for REE Pre-Concentration and Downstream Extraction

The central finding of this study is that dry electrostatic and magnetic separation can provide useful process-response information on REE partitioning but did not generate a favourable combination of enrichment factor and product yield for the investigated low-grade, heterogeneous materials.

The combined EF–yield assessment confirms that none of the tested configurations produced the desired combination of high enrichment factor and high product yield. Electrostatic separation produced selected moderate enrichment effects, whereas magnetic separation was characterized by very low yields of magnetically susceptible products and frequent ΣREE depletion. This indicates that the investigated dry separation methods had limited potential for effective REE pre-concentration under the applied laboratory conditions.

This result is particularly relevant for low-grade coal-derived waste streams, where moderate enrichment factors do not necessarily translate into process-relevant concentrates. At feed concentrations of 109.33–250.54 ppm ΣREE, EF values close to unity, or even moderately above unity, remain insufficient unless they are accompanied by meaningful product yield and mass-based REE recovery. For example, an EF of 1.26 or 1.30 may indicate preferential partitioning, but it does not by itself demonstrate a practically useful

concentration effect if the resulting product mass is low or if the absolute REE concentration remains limited.

The results therefore show that product yield and material heterogeneity are as important as the enrichment factor itself. In the electrostatic tests, the most promising responses were material-specific and moderate. In the magnetic tests, selected products showed elevated EF values, but their low yields limited their practical significance. These findings indicate that dry separation can provide useful screening information on REE partitioning, but downstream extraction studies should be prioritized only for fractions that combine enrichment with sufficient product mass and favourable chemical characteristics.

The role of dry separation in this context is best understood as a preliminary process-response screening step. Such screening can help determine whether REE-bearing components are preferentially associated with electrically or magnetically distinguishable fractions before more selective extraction methods, such as chemical leaching or bioleaching, are applied. In the present study, the weak EF–yield relationships indicate that dry separation alone is unlikely to provide substantial mass reduction before downstream REE extraction for most of the investigated materials.

The practical interpretation of these results is limited by the laboratory scale of the tests and by the absence of downstream extraction, techno-economic and environmental assessments. Electricity demand, equipment scale-up, reagent use in subsequent extraction, product handling and overall process costs were not evaluated. Therefore, further work should combine process-response screening with mineralogical characterization, mass-based REE recovery calculations, downstream extraction tests, and techno-economic and environmental evaluation.

The scientific value of the study therefore lies in defining the practical boundary conditions for dry physical separation before downstream REE extraction is considered. The results show that enrichment factors must be evaluated together with product yield, material heterogeneity and absolute REE concentration. In this role, dry separation is useful primarily as a comparative screening step for identifying whether selected waste streams or separated products justify further mineralogical characterization and downstream extraction testing.

5. Conclusions

This study compared the response of five coal-derived post-mining waste streams from Poland and the Czech Republic to dry electrostatic and magnetic separation, with a focus on REE partitioning behaviour, enrichment factor and product yield.

The investigated materials showed substantial heterogeneity in ΣREE content, LOI and separation response. The ΣREE content of the feeds ranged from 109.33 ppm in Haldex K to 250.54 ppm in Haldex O, confirming that bulk REE concentration alone is insufficient for assessing beneficiation potential.

Electrostatic separation produced only moderate and material-specific REE enrichment. Most products showed EF ΣREE values close to unity, while the highest and most consistent response was observed for the Haldex K conductive product from Test II, where EF ΣREE reached 1.26 with simultaneous enrichment of Nd, Pr and Dy.

Magnetic separation showed a less favourable response. Most magnetically susceptible products were depleted in ΣREE relative to the feed. Although the Haldex K paramagnetic product reached EF ΣREE = 1.30 and EF Dy = 1.76, its yield was only 0.2%, which strongly limits the practical significance of this enrichment.

No tested configuration combined high REE enrichment with high product yield. The main contribution of this study is the comparative evaluation of REE partitioning behaviour during dry electrostatic and magnetic separation of five heterogeneous coal-derived post-

mining waste streams. The results identify the main limitations of dry physical separation for low-grade materials, including moderate enrichment factors, low or unfavourable product yields, material-dependent response and the need to interpret EF values together with mass distribution. These findings define dry separation primarily as a preliminary process-response screening tool for assessing whether selected waste streams or separated products justify further downstream extraction studies.

Supplementary Materials: The following supporting information can be downloaded at: https://www.mdpi.com/article/10.3390/min16060604/s1, Table S1: Technical specifications of the electrostatic separator; Table S2: Operating parameters of the electrostatic separation process; Table S3: Feed mass used for electrostatic separation; Table S4: Technical specifications of the plate-type magnetic separator; Table S5: Feed mass used for magnetic separation; Table S6: Operating parameters of the magnetic separator; Table S7: Samples obtained during magnetic separation; Table S8: Feed sample identification; Table S9: Full chemical composition of electrostatic separation products; Table S10: Full chemical composition of magnetically susceptible products.

Author Contributions: Conceptualization, P.F., D.K. and P.M.; methodology, P.F., D.K. and P.M.; formal analysis, P.F., R.B., A.C. and K.I.; investigation, P.F., R.B. and O.Z.; resources, P.F., R.B., D.K., P.M. and O.Z.; data curation, P.F. and R.B.; visualization, P.F., R.B. and O.Z.; writing—original draft preparation, P.F. and D.K.; writing—review and editing, P.F., R.B., D.K., P.M., O.Z., A.C. and K.I.; validation, P.F., D.K., P.M. and A.C.; supervision, D.K. and P.M.; project administration, P.M. and K.I. All authors have read and agreed to the published version of the manuscript.

Funding: This research was co-funded by the European Commission within the framework of the Research Fund for Coal and Steel (RFCS) program under contract no. 101112386 and by a state subsidy, contract no. 5676/FBWiS/2023/2024/2, within the framework of the program 'Co-financed International Projects' (PMW) established by the Minister of Science and Higher Education of Poland. The APC was also funded by these sources.

Data Availability Statement: The original contributions presented in this study are included in the article/Supplementary Material. Further inquiries can be directed to the corresponding author.

Conflicts of Interest: The authors declare no conflicts of interest. The funders had no role in the design of the study; in the collection, analyses, or interpretation of data; in the writing of the manuscript; or in the decision to publish the results.

Abbreviations

The following abbreviations are used in this manuscript:

REE	rare earth elements
ΣREE	total rare earth elements
ΣLREE	total light rare earth elements
ΣHREE	total heavy rare earth elements
EF	enrichment factor
LOI	loss on ignition
SD	standard deviation
RSD	relative standard deviation
DL	limit of detection (reported as <DL)
ICP-MS	inductively coupled plasma mass spectrometry
RH	relative humidity
DC	direct current
CRM	critical raw materials
ISO	International Organization for Standardization
EU	European Union

References

1. International Energy Agency. *Executive Summary: Global Critical Minerals Outlook 2025–Analysis*; International Energy Agency: Paris, France, 2025.
2. Cheilas, P.; Christou, T.; Karkalakos, S.; Kottaridi, C.; Michaelides, P.G. Rare Earth Elements and the US Renewable Economy: A Causality Exploration between Critical Materials and Clean Energy. *Resour. Policy* **2025**, *101*, 105491. [CrossRef]
3. García-Gusano, D.; Iribarren, D.; Muñoz, I.; Arrizabalaga, E.; Mabe, L.; Martín-Gamboa, M. The Future Need for Critical Raw Materials Associated with Long-Term Energy and Climate Strategies: The Illustrative Case Study of Power Generation in Spain. *Energy* **2025**, *314*, 134266. [CrossRef]
4. Liu, Q.; Sun, K.; Ouyang, X.; Sen, B.; Liu, L.; Dai, T.; Liu, G. Tracking Three Decades of Global Neodymium Stocks and Flows with a Trade-Linked Multiregional Material Flow Analysis. *Environ. Sci. Technol.* **2022**, *56*, 11807–11817. [CrossRef] [PubMed]
5. OJEU. *Regulation (EU) 2024/1252 Establishing a Framework for Ensuring a Secure and Sustainable Supply of Critical Raw Materials (Critical Raw Materials Act)*; OJEU: Luxembourg, 2024; Volume 2024/1252.
6. Pimenow, S.; Pimenowa, O.; Rembisz, W. Circular Economy Pathways for Critical Raw Materials: European Union Policy Instruments, Secondary Supply, and Sustainable Development Outcomes. *Sustainability* **2026**, *18*, 562. [CrossRef]
7. United Nations Goal 12: Responsible Consumption and Production. Available online: https://globalgoals.org/goals/12-responsible-consumption-and-production/ (accessed on 2 February 2026).
8. Kirchherr, J.; Reike, D.; Hekkert, M. Conceptualizing the Circular Economy: An Analysis of 114 Definitions. *Resour. Conserv. Recycl.* **2017**, *127*, 221–232. [CrossRef]
9. With New Export Controls on Critical Minerals, Supply Concentration Risks Become Reality–Analysis. Available online: https://www.iea.org/commentaries/with-new-export-controls-on-critical-minerals-supply-concentration-risks-become-reality (accessed on 2 February 2026).
10. Imports of Rare Earth Elements Saw 30% Drop in 2024. Available online: https://ec.europa.eu/eurostat/web/products-eurostat-news/w/ddn-20250409-1 (accessed on 2 February 2026).
11. Matusiak, P. Use of State-of-the-Art Jigs of KOMAG Type for a Beneficiation of Coking Coal. *Min. Mach.* **2020**, *161*, 46–55. [CrossRef]
12. Gawor, Ł. Coal Mining Waste Dumps as Secondary Deposits–Examples from the Upper Silesian Coal Basin and the Lublin Coal Basin. *Geol. Geophys. Environ.* **2014**, *40*, 285. [CrossRef]
13. Kowol, D.; Matusiak, P.; Baron, R.; Friebe, P.; Jendrysik, S.; Bigda, J.; Czardybon, A.; Ignasiak, K. Application of Jigging Beneficiation for Processing of Waste from Post-Mining Heaps for Circular Economy Purposes. *Minerals* **2025**, *15*, 1108. [CrossRef]
14. Kowol, D.; Matusiak, P.; Palou, M.T.; Kielar, J. Design and Application Development of KOMAG-Type Pulsating Concentrators. *Min. Mach.* **2026**, *44*, 1–11. [CrossRef]
15. Friebe, P.; Baron, R.; Matusiak, P.; Kowol, D. *New Technology for Hydrogen and Geopolymer Composites Production from Post-Mining Waste; WP5: Development of Methods of Using the Mineral Wastes from Jig Beneficiation Process—Chemical Composition Analysis of Post-Mining Waste*; ITG KOMAG: Gliwice, Poland, 2025.
16. Baioumy, H.; Ulfa, Y.; Nawawi, M.; Padmanabhan, E.; Anuar, M.N.A. Mineralogy and Geochemistry of Palaeozoic Black Shales from Peninsular Malaysia: Implications for Their Origin and Maturation. *Int. J. Coal Geol.* **2016**, *165*, 90–105. [CrossRef]
17. Thomas, B.S.; Dimitriadis, P.; Kundu, C.; Vuppaladadiyam, S.S.V.; Raman, R.K.S.; Bhattacharya, S. Extraction and Separation of Rare Earth Elements from Coal and Coal Fly Ash: A Review on Fundamental Understanding and on-Going Engineering Advancements. *J. Environ. Chem. Eng.* **2024**, *12*, 112769. [CrossRef]
18. Fu, B.; Hower, J.C.; Zhang, W.; Luo, G.; Hu, H.; Yao, H. A Review of Rare Earth Elements and Yttrium in Coal Ash: Content, Modes of Occurrences, Combustion Behavior, and Extraction Methods. *Prog. Energy Combust. Sci.* **2022**, *88*, 100954. [CrossRef]
19. Hussain, Z.; Dwivedi, D.; Kwon, I. Recovery of Rare Earth Elements from Low-Grade Coal Fly Ash Using a Recyclable Protein Biosorbent. *Front. Bioeng. Biotechnol.* **2024**, *12*, 1385845. [CrossRef]
20. Dascalescu, L.; Zeghloul, T.; Medles, K.; Iuga, A. Recent Advances in the Electrostatic Separation of Particulate Matter. *J. Electrost.* **2025**, *134*, 104036. [CrossRef]
21. Zhao, R.; Zhang, Z.; Bai, X.; Wang, H.; Zhang, H.; Hao, J.; Wang, C. A Review of the Research on Triboelectric Separation Technology. *Miner. Eng.* **2024**, *216*, 108901. [CrossRef]
22. Tripathy, S.K.; Banerjee, P.K.; Suresh, N.; Murthy, Y.R.; Singh, V. Dry High-Intensity Magnetic Separation In Mineral Industry—A Review Of Present Status And Future Prospects. *Miner. Process. Extr. Metall. Rev.* **2017**, *38*, 339–365. [CrossRef]
23. Vilakazi, A.Q.; Shemi, A.; Ndlovu, S. Dry Magnetic Separation and the Leaching Behaviour of Aluminium, Iron, Titanium, and Selected Rare Earth Elements (REEs) from Coal Fly Ash. *Minerals* **2025**, *15*, 119. [CrossRef]

24. Bishop, B.A.; Shivakumar, K.R.; Alessi, D.S.; Robbins, L.J. Insights into the Rare Earth Element Potential of Coal Combustion By-Products from Western Canada. *Environ. Sci. Adv.* **2023**, *2*, 529–542. [CrossRef]
25. *ISO 18400-101:2017*; Soil quality—Sampling—Part 101: Framework for the preparation and application of a sampling plan. International Organization for Standardization: Geneva, Switzerland, 2017.